Band structure effects on one-dimensional resonant tunneling in STM tips made of carbon nanotubes

Jinhua Gao,[1] Qingfeng Sun,[1] X. C. Xie,[1,2] and Hongjun Gao[1]
[1]*Institute of Physics, Chinese Academy of Science, Beijing 100080, China*
[2]*Department of Physics, Oklahoma State University, Stillwater, Oklahoma 74078, USA*
(Received 10 November 2005; revised manuscript received 25 April 2006; published 21 June 2006)

In recent experiments, attempts were made to use carbon nanotubes to replace the normal metal tips in the scanning tunneling microscope (STM), and stable atomic images were observed. However, does the one-dimensional characteristic band structure of the carbon nanotube (CNT) affect the tunneling? We present a theoretical analysis of the one-dimensional resonance tunneling model using the nonequilibrium Green's function method. The results clearly imply that the Van Hove singularities of the CNT probe play an important role in the tunneling process. The resonance curve is quite different from the one with a metallic tip; new peaks and peak splittings are induced. So these characteristics must be considered seriously if one uses a nanoprobe as the STM tip. We also notice that a sharp peak will appear near the first Van Hove singularity, which resembles the Kondo peak.

DOI: 10.1103/PhysRevB.73.235421 PACS number(s): 73.23.−b, 68.37.Ef

Because of the small tip radius, chemical inertness, intrinsic electronic conductivity, and mechanical resilience, carbon nanotubes (CNTs) are quite suitable to be used as the tips of the scanning probe microscope.[1] They have already been successfully used as tips of the atomic force microscope,[2] and recently attempts were made to attach them to the very end of the normal metal tip of the scanning tunneling microscope (STM) to construct a nanoprobe of the STM.[3–5] Stable atomic images have already been observed. Meanwhile, it is expected that this kind of nanoprobe can be used in a multiprobe STM system to measure the electronic transport properties of nanostructure systems.[6]

However, unlike the common metal tips, CNTs have characteristic one-dimensional electronic structure. They have a very specific band structure consisting of many one-dimensional subbands. The spacing of these subbands depends on the diameter and the chirality of the nanotube.[7,8] A recent experiment[9] demonstrated that the band structure of the nanotube does affect the transport property, especially near the Van Hove singularities. Thus, whether a nanoprobe is used as an electrode in a transport measurement, or as an STM tip, one needs to pay attention to the effects of one-dimensional band structure.

In this work, we use the nonequilibrium Green's function method[10–13] to analyze the resonance tunneling process in a STM that uses a carbon nanotube as its tip. The results imply that the Van Hove singularities of the density of states, which result from the characteristic one-dimensional band structure, have profound impact on the resonance tunneling. The scanning tunneling spectroscopy will be greatly changed. These phenomena can be observed experimentally, and must be considered seriously if a nanoprobe is employed as a STM tip.

The method used in this study is discussed in detail in Ref. 13. The main difference is that the normal lead is replaced by the nanotube. We attempt to see how the Van Hove singularities in the density of states (DOS) of the nanotube influence the tunneling processes.

A typical experimental geometry is sketched in Fig. 1, in which a CNT probe attached to the end of a metallic STM tip couples to a molecule on the substrate. The total Hamiltonian contains three pieces, $H=H_c+H_T+H_{\mathrm{cen}}$, where H_c describes the contacts (i.e., probe and the substrate), H_T is the tunneling coupling between the central region (i.e., molecule) and the contacts, and H_{cen} represents the central region.

The electrons in the contacts (both probe and substrate) are viewed as noninteracting. We can write the Hamiltonian as

$$H_c = \sum_{\substack{k\in S,P \\ \sigma}} \epsilon_{k\sigma} c_{k\sigma}^{+} c_{k\sigma}. \tag{1}$$

Here, $c_{k\sigma}$ and $c_{k\sigma}^{+}$ are the creation and annihilation operators for the free electrons in the nanoprobe and substrate. The indices S and P represent the substrate and probe, respectively. The main difference between the substrate and the probe is their DOS. The DOS of the substrate can be viewed as a constant as usual, but the probe is now quasi-one-dimensional and the one-dimensional DOS must be used here. Detailed calculation of the one-dimensional DOS with Van Hove singularities is well known.[14] From these data [e.g., see Fig. 2(a)], we can see that for a typical CNT there will be two or three Van Hove singularities in the energy interval that ranges from normal Fermi energy to 2 eV above

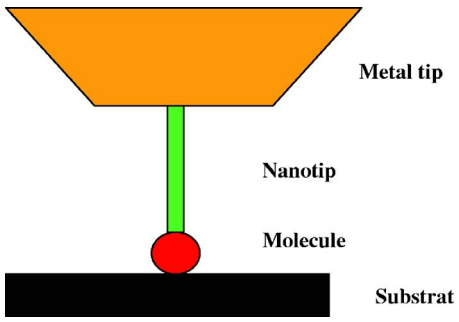

FIG. 1. (Color online) The sketch map of the STM system with a carbon nanotube as its tip.

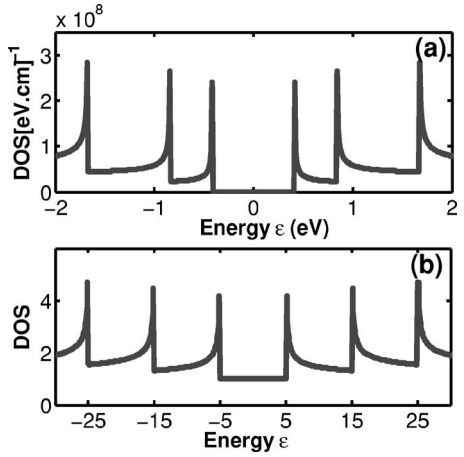

FIG. 2. (a) The DOS of carbon nanotube (13,0). (b) The DOS of a nanoprobe calculated with Eq. (5) and the parameter $\alpha=1$.

or below it. The Fermi energy of the nanoprobe can be shifted up or down if we apply positive or negative voltage between the tip and the substrate. In STM measurement, scanning voltage is usually between ±2 eV. Thus in an experiment the Fermi level of the nanoprobe will be shifted through several subbands or Van Hove singularities. Since the nanoprobe is attached to the very end of the metal tip, they will be considered as a whole, which serves as the electron reservoir and always in equilibrium.

We do not want to dwell on the detail band structure of these CNT probes. Different chirality has different band structures, and the positions of the Von Hove singularities are also different.[14] Our main purpose here is to see how the band structures affect the tunneling, therefore the band structure of a quasi-one-dimensional quantum wire with the harmonic confined potential is used to mimic that of the nanoprobe. The energy spectrum of the quasi-one-dimensional probe is

$$E_j(k) = E_j + \frac{\hbar^2 k^2}{2m^*}, \tag{2}$$

$$E_j = \hbar\,\omega_0\left(j + \tfrac{1}{2}\right). \tag{3}$$

Then the DOS of the probe is taken as

$$D_p(E) = D_0 + D_j(E) = D_0 + \alpha\sum_{j=0}\frac{\theta(E-E_j)}{\sqrt{E-E_j}}, \quad E \geq 0,$$

$$D_p(E) = D_P(-E), \quad E < 0, \tag{4}$$

where $\alpha=(1/\pi)(2m^*/\hbar^2)^{1/2}$. Figures 2(a) and 2(b) show the DOS compared with that of the CNT. If the D_0 is a nonzero constant, it implies that the CNT is metallic. Otherwise, if $D_0=0$, it has the semiconducting behavior. The spacing between two subbands is determined by the width of the nanowire. In an experiment, it depends on the chirality and diameter of the CNT. From Figs. 2(a) and 2(b), we can see that the mock DOS we used here is quite similar to the DOS of the CNT. Therefore, this assumption is reasonable.

The Hamiltonian of the central region (we can take it as a molecule) is

$$H_{\text{cen}} = \sum_{\sigma} \epsilon_d d_\sigma^+ d_\sigma, \tag{5}$$

where d_σ^+ and d_σ are the creation and annihilation operators for the discrete energy level with the spin σ in the molecule. Here, we do not consider the Coulomb interaction in the central region, and this case will be considered later. Therefore, it presents a simple model for resonance tunneling, and only one discrete energy level is considered here.

The tunneling coupling Hamiltonian H_T is

$$H_T = \sum_{\substack{k\in S,P \\ \sigma}} (V_{k\sigma} c_{k\sigma}^+ d_\sigma + \text{H.c}). \tag{6}$$

Here $V_{k\sigma}$ are the coupling constants between the contacts and the central region, which depend on the superposition of their wave functions and need to be computed self-consistently. In our calculations, we assume that these parameters are constants. From an experimental point of view, one can adjust the coupling constant $V_{k\sigma}$ between the nanoprobe and the central region (i.e., molecule) by changing the distance between them.

The above model can be solved exactly. Since both the conductance dI/dV and the local DOS relate to the Green's function of the molecule, we first solve the retarded Green's function $G_\sigma^r(\epsilon)$ by using the Dyson equation,

$$G_\sigma^r(\epsilon) = g_\sigma^r(\epsilon) + g_\sigma^r(\epsilon)\Sigma_\sigma^r(\epsilon)G_\sigma^r(\epsilon). \tag{7}$$

Here $G_\sigma^r(\epsilon)$ is the Fourier transformation of $G_\sigma^r(t)$, and $G_\sigma^r(t) \equiv -i\theta(t)\langle\{d_\sigma(t), d_\sigma^+(0)\}\rangle$. $g_\sigma^r(\epsilon)$ is the molecular Green's function without coupling between the contacts and the molecule (i.e., when $V_{k\sigma}=0$). $g_\sigma^r(\epsilon)$ can be solved exactly as

$$g_\sigma^r(\epsilon) = \frac{1}{\epsilon - \epsilon_d + i\eta}, \tag{8}$$

where η is a very small positive number. The retarded self-energy $\Sigma_\sigma^r(\epsilon)$ in Eq. (7) is of the form

$$\Sigma_\sigma^r(\epsilon) = \sum_{k\in S,P} |V_{k\sigma}|^2 g_{k\sigma}^r(\epsilon) = \Sigma_{\sigma S}^r(\epsilon) + \Sigma_{\sigma P}^r(\epsilon), \tag{9}$$

with $g_{k\sigma}^r(\epsilon)=1/(\epsilon-\epsilon_{k\sigma}+i\eta)$. Since the DOSs of the substrate and that of the probe are different, we have to treat the two retarded self-energies, respectively. Take the probe's retarded self-energy $\Sigma_{\sigma P}^r(\epsilon)$, for example,

$$\Sigma_{\sigma P}^r(\omega) = \sum_{k\in P}\frac{|V_{k\sigma}|^2}{\omega-\epsilon_{k\sigma}+i\eta} = \sum_{k\in P}\int d\epsilon \frac{|V_{k\sigma}|^2\delta(\epsilon-\epsilon_{k\sigma})}{\omega-\epsilon+i\eta}$$
$$= R_{\sigma P}^r(\omega) + iI_{\sigma P}^r(\omega), \tag{10}$$

where

$$R_{\sigma P}^r(\omega) = P\int d\epsilon \frac{\sum_{k\in P}|V_{k\sigma}|^2\delta(\epsilon-\epsilon_{k\sigma})}{\omega-\epsilon} = P\int \frac{d\epsilon}{2\pi}\frac{\Gamma_{\sigma P}^r(\epsilon)}{\omega-\epsilon}, \tag{11}$$

$$I^r_{\sigma P}(\omega) = -\frac{\Gamma^r_{\sigma P}(\omega)}{2}, \tag{12}$$

and $\Gamma^r_{\sigma P}(\epsilon) \equiv 2\pi\Sigma_{k\in P}|V_{k\sigma}|^2\ \delta(\epsilon-\epsilon_{k\sigma})$. Up to now, all the formalisms have been exact; no approximation has been used. Now we take the assumption that $V_{k\sigma}$ is a constant, so $\Gamma^r_{\sigma P}(\epsilon)$ reduces to

$$\Gamma^r_{\sigma P}(\epsilon) = 2\pi|V_{\sigma P}|^2\sum_{k\in P}\delta(\epsilon-\epsilon_{k\sigma}) = 2\pi|V_{\sigma P}|^2 D_{\sigma P}(\epsilon). \tag{13}$$

If the probe is a normal metal tip, we can regard the DOS as a constant; then $\Gamma^r_{\sigma P}(\epsilon)$ is also a constant. But when we consider the CNT nanoprobe, the one-dimensional DOS has to be used. In the following calculation, the mimic DOS $D_{\sigma P}(\epsilon)$ of Eq. (4) is used, in which the $D_{\sigma P}(\epsilon)$ is an even function. To compare with the detailed data of the DOS of the CNT in Ref. 14, this hypothesis is quite reasonable. From an even function of $D_{\sigma P}(\epsilon)$, it is straightforward to prove $I^r_{\sigma P}(-\epsilon) = I^r_{\sigma P}(\epsilon)$ and $R^r_{\sigma P}(-\epsilon) = -R^r_{\sigma P}(\epsilon)$. These relations can greatly simplify the calculation. Figures 3(a) and 3(b) show the imaginary part $I^r_{\sigma P}(\epsilon)$ and real part $R^r_{\sigma P}(\epsilon)$ of the self-energy, respectively. Both the imaginary part $I^r_{\sigma P}(\epsilon)$ and real part $R^r_{\sigma P}(\epsilon)$ exhibit Van Hove singularities. This result is quite different from that of a normal contact with a constant DOS. In the latter case, the imaginary part is a constant $-\Gamma^r/2$ and the real part is quite small, so that we consider it as zero.

Next, we calculate the substrate's retarded self-energy $\Sigma^r_{\sigma S}(\epsilon)$. Here, we point out that the self-energy function $\Sigma^r_{\sigma S}(\epsilon)$ can be absorbed in $\Sigma^r_{\sigma P}(\epsilon)$ during the calculation. Then the real part $R^r_\sigma(\epsilon)$ and the imaginary part $I^r_\sigma(\epsilon)$ of the total self-energy are

$$\begin{aligned} R^r_\sigma(\omega) &= R^r_{\sigma P}(\omega) + R^r_{\sigma S}(\omega) \\ &= |V_{P,\sigma}|^2 P\int_{-D}^{D} d\epsilon \frac{D_{\sigma P}(\epsilon)}{\omega-\epsilon} + |V_{S,\sigma}|^2 P\int_{-D}^{D} d\epsilon \frac{D_{\sigma S}(\epsilon)}{\omega-\epsilon} \\ &= |V_{P,\sigma}|^2 P\int_{-D}^{D} d\epsilon \frac{(D_0+\beta D_{\sigma S}) + \sum_j D_j(\epsilon)}{\omega-\epsilon} \\ &= |V_{P,\sigma}|^2 P\int_{-D}^{D} d\epsilon \frac{D_0' + \sum_j D_j(\epsilon)}{\omega-\epsilon}, \end{aligned} \tag{14}$$

$$\begin{aligned} I^r_{\sigma S}(\omega) + I^r_{\sigma P}(\omega) &= -\frac{\Gamma^r_{\sigma S}(\omega) + \Gamma^r_{\sigma P}(\omega)}{2} \\ &= -\pi|V_{\sigma S}|^2 D_{\sigma S}(\omega) - \pi|V_{\sigma P}|^2 D_{\sigma P}(\omega) \\ &= -\pi|V_{\sigma P}|^2\left[D_0' + \sum_j D_j(\omega)\right], \end{aligned} \tag{15}$$

where $D_0' = D_0 + \beta D_{\sigma S}$ and $\beta \equiv |V_{S,\sigma}|^2/|V_{P,\sigma}|^2$. In general, the coupling between the molecule and the substrate is not too strong, so that β is not a large number.

After solving the retarded self-energy $\Sigma^r_\sigma(\epsilon)$, the retarded Green's function can be obtained straightforwardly, $G^r_\sigma(\epsilon) = 1/(g^{r-1}_\sigma - \Sigma^r_\sigma)$. Then the local DOS of the molecule $\rho(\epsilon)$ is

$$\begin{aligned} \rho(\epsilon) &= -\frac{1}{\pi}\,\mathrm{Im}\,G^r_d(\epsilon) = -\frac{1}{\pi}\frac{I(\epsilon)}{[\epsilon-\epsilon_d-R(\epsilon)]^2 + I(\epsilon)^2} \\ &\equiv -\frac{1}{\pi}\frac{I(\epsilon)}{A(\epsilon)^2 + I(\epsilon)}. \end{aligned} \tag{16}$$

In this formula, we neglect the spin indices. We define $A(\epsilon) \equiv \epsilon - \epsilon_d - R(\epsilon)$, which helps us to describe our results.

In the numerical calculations, we take $V_p = 1$ as an energy unit, and $D_0' = \beta D_{\sigma S} + D_0 = 1$. D_0 and $D_{\sigma S}$ are determined by the nanoprobe and substrate themselves. The only changeable parameter is β, i.e., the ratio of the coupling constant of the substrate to that of the nanoprobe. The concrete shape of the DOS $\rho(\epsilon)$ of the resonance depends on the position of the molecular energy level ϵ_d. Because both the imaginary and real parts of the self-energy have Van Hove singularities, the real part cannot be neglected any more, and the imaginary part also has a different effect. When the discrete molecular level ϵ_d approaches the singularities, their influences show up in the DOS of the molecule.

Figures 4(a) and 4(c) show several typical results of the DOS $\rho(\epsilon)$. If the probe is a normal metal tip and the DOS of probe is a constant, the local DOS $\rho(\epsilon)$ of the molecule is Lorentz form, shown as the dash-dotted curve in Fig. 4(a). However, while the probe is a quasi-one-dimensional CNT nanoprobe and its DOS $D_P(\epsilon)$ has Van Hove singularities, the local DOS $\rho(\epsilon)$ is strongly affected [see the solid curve in Fig. 4(a)]. In order to investigate the effect in detail, we first set the imaginary part $I^r(\epsilon)$ of the self-energy to a constant; the effects of the real part $R^r(\epsilon)$ can then be understood through the function $A(\epsilon)$. Take $\epsilon_d = 17$, which is near the second Van Hove singularity, for example; $A(\epsilon)$ has two zero points and two singularities [see Fig. 4(b)]. The zero points give two peaks in the DOS $\rho(\epsilon)$ [see Fig. 4(a)]. The first singularity induces a sharp peak, while the second one gives a splitting. Then we turn on the imaginary part $I^r(\epsilon)$. Due to its asymmetry around the second singularity, the two peaks induced by the zero points are reduced differently. Different from this case, when the discrete energy level of the mol-

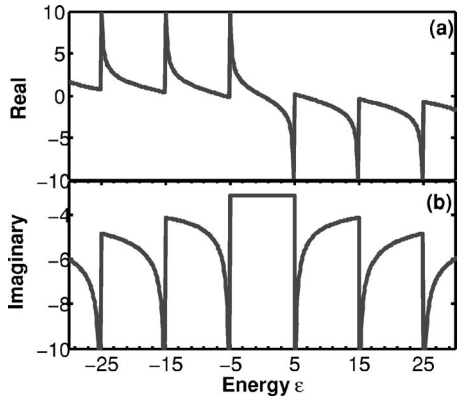

FIG. 3. (a) The real part of the self-energy calculated with formula (14). $D=500$, $D_0'=1$, $|V_{\sigma P}|=1$. (b) The image part of the self-energy calculated with formula (15). $D=500$, $D_0'=1$, $|V_{\sigma P}|=1$.

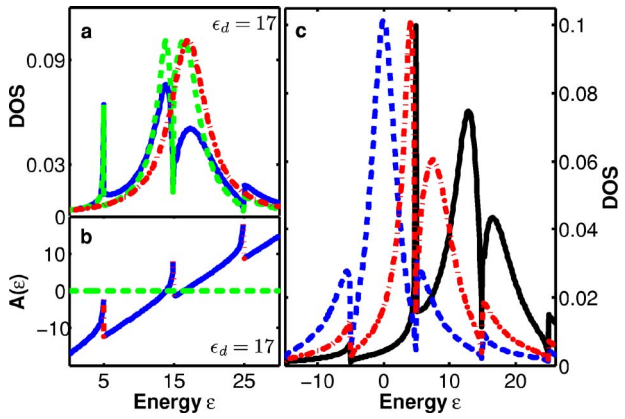

FIG. 4. (Color online) (a) The solid line: the local DOS of the single energy level molecule when ϵ_d=17. The dashed line: the local DOS of the single energy level molecule when ϵ_d=17, but the image part of the self-energy is set to be a constant $-\pi$. The dash-dotted line: the local DOS of the single energy level molecule when ϵ_d=17, but the DOS of the probe is constant (normal metal tip). (b) The assistant function $A(\epsilon)$ when ϵ_d=17. (c) The local DOS of the single energy level molecule when ϵ_d=0 (dashed line), ϵ_d=7 (red, dash-dot line), ϵ_d=15 (solid line).

ecule is around the first Van Hove singularity, the singularity itself will not induce any peak but only a splitting, which is shown clearly in Fig. 4(c).

We also notice that the sharp peak induced by the first singularity is quite similar to the Kondo peak in appearance, i.e., a sharp peak on a broad shoulder. But they are different in essence. The Kondo peak is always at the Fermi energy, and one can see it with a small voltage. But the Van Hove peak is always at the Van Hove singularity; one must use a large voltage to shift the Fermi energy level through the singularities. The Kondo peak results from the Coulomb interaction in the molecule, but in our model the peak is from the Van Hove singularity, which has nothing to do with the Coulomb interaction.

Next, we calculate the current-voltage curve. From the retarded Green's function, the current I is easily obtained as[13]

$$I = \frac{4e}{\hbar}\int \frac{d\epsilon}{2\pi}\frac{I_P^r(\epsilon)I_S^r(\epsilon)}{[\epsilon-\epsilon_d-R^r(\epsilon)]^2+I^r(\epsilon)^2}[f_P(\epsilon)-f_S(\epsilon)], \tag{17}$$

where $f_{P/S}(\epsilon)=1/\{\exp[(\epsilon-\mu_{P/S})/k_BT]+1\}$ are the Fermi distribution functions of the probe and substrate, respectively, with the chemical potential (Fermi energy level) μ_P, μ_S and the bias voltage $V=\mu_P-\mu_S$. In the following, we only consider the zero-temperature case. Thus the current I and the conductance dI/dV reduce to

$$I = \frac{4e}{\hbar}\int_{\mu_S}^{\mu_P}\frac{d\epsilon}{2\pi}\frac{I_{\sigma P}^r(\epsilon)I_{\sigma S}^r(\epsilon)}{[\epsilon-\epsilon_d-R^r(\epsilon)]^2+I^r(\epsilon)^2}, \tag{18}$$

$$\frac{dI}{dV}(\mu_P) = \frac{2e}{\hbar\pi}\frac{I_{\sigma P}^r(\mu_P)I_{\sigma S}^r(\mu_P)}{[\mu_P-\epsilon_d-R^r(\mu_P)]^2+I^r(\mu_P)^2}. \tag{19}$$

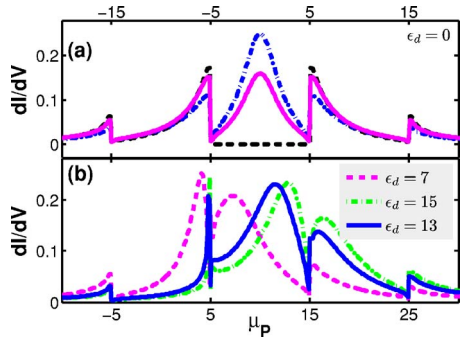

FIG. 5. (Color online) (a) The dI/dV curves of the case ϵ_d=0: $\beta D_{\sigma S}$=1, D_0=0 (dashed line); $\beta D_{\sigma S}$=0.5, D_0=0.5 (dash-dotted line); $\beta D_{\sigma S}$=0.8, D_0=0.2 (solid line). (b) The dI/dV curves of the case $\beta D_{\sigma S}$=0.5: ϵ_d=15 (dash-dotted line); ϵ_d=13 (solid line); ϵ_d=7 (dashed line).

Figures 5(a) and 5(b) show the conductance dI/dV versus the chemical potential of the nanoprobe μ_P. The shape of the dI/dV curve resembles the DOS, the only difference being the amplitude. When $\beta D_{\sigma S}$ approaches 0.5, the amplitude reaches its maximum. On the other hand, if $\beta D_{\sigma S}$ is 1, the conductance dI/dV reaches zero while the energy ϵ_F is near zero [see Fig. 5(a)], because with this parameter value the nanotube is a semiconductor with D_0=0. In an experiment, the parameter $\beta D_{\sigma S}$ can be tuned by changing the distance between the nanoprobe and the molecule. We emphasize that the conductance dI/dV for the CNT probe is quite different in comparison to the probe being a normal metal tip; in the latter case, the conductance curve looks like the dashed curve in Fig. 6(a).

The dI/dV curve is also a function of the coupling constant V_P that depends on the distance between the probe and molecule. From Fig. 6(c), we can see clearly that it is not a monotonic relation. If we assume that the coupling between the probe and the molecule is stronger when we decrease the distance between them, the relation between dI/dV and the distance between the probe and the molecule is also a nonmonotonic one.

In the normal scanning process, the voltage between the substrate and the probe is fixed and usually not too large

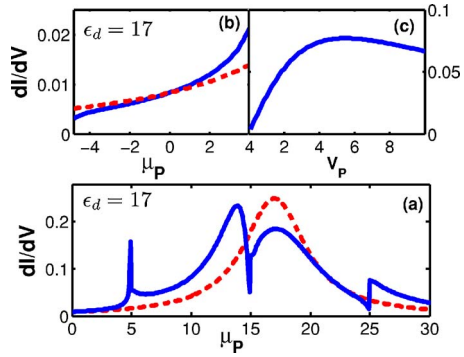

FIG. 6. (Color online) (a) The dI/dV curves of the case ϵ_d=17 (solid line); the dI/dV curves of normal tip (dashed line). (b) The detail structure of the dI/dV curves (a) in the range of small voltage. (c) The relation between dI/dV curves and coupling constant V_p.

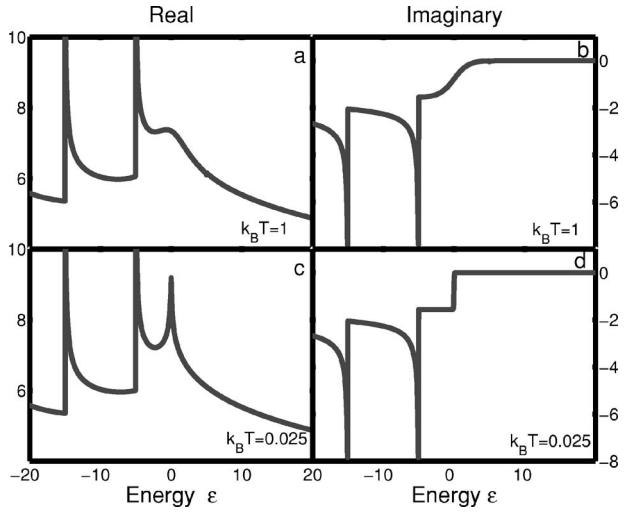

FIG. 7. (a) The real part of the self-energy $\Sigma^r_{1\sigma}(\omega)$, $k_BT=1$, $D=500$, $D'_0=1$, $|V_{\sigma P}|=0.5$; (b) the imaginary part of the self-energy $\Sigma^r_{1\sigma}(\omega)$, $k_BT=1$, $D=500$, $D'_0=1$, $|V_{\sigma P}|=0.5$; (c) the real part of the self-energy $\Sigma^r_{1\sigma}(\omega)$, $k_BT=0.025$, $D=500$, $D'_0=1$, $|V_{\sigma P}|=0.5$; (d) the imaginary of the self-energy $\Sigma^r_{1\sigma}(\omega)$, $k_BT=0.025$, $D=500$, $D'_0=1$, $|V_{\sigma P}|=0.5$.

(below 2 eV). When the scanning voltage is below the first Van Hove singularity, the imaginary part of the self-energy is a constant (Fig. 3). The difference between the CNT probe and the normal probe only results from the real part. But the real part is an odd function, so the current difference in this range will be greatly canceled [see Fig. 6(b)]. In other words, if the scanning voltage is below the first Van Hove singularity, there will be no difference in the scanning image with a CNT probe or with a normal metal probe.

The analyses above are for the noninteracting case. This means that we did not consider the Coulomb interaction in the molecule. With interaction, the Hamiltonian of the central region is changed to

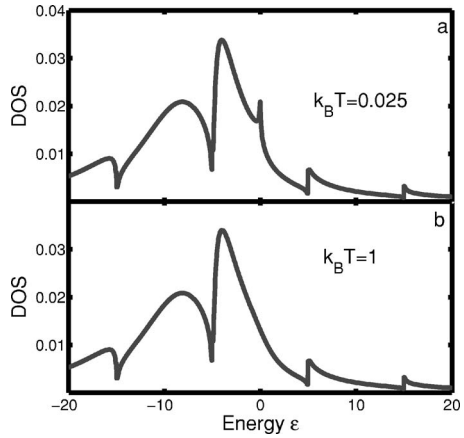

FIG. 8. (a) The local DOS of the single energy level molecule when $\epsilon_d=-13$, $k_BT=0.025$; (b) the local DOS of the single energy level molecule when $\epsilon_d=-13$, $k_BT=1$.

$$H_{\text{cen}}=\sum_{\sigma}\epsilon_d d^+_\sigma d_\sigma + U n_\uparrow n_\downarrow,$$

where U is the Coulomb-interaction energy between the two on-site electrons. For simplicity, we only consider the zero-magnetic-field case and set $U=\infty$. We will show that our analyses are also suitable for the interacting case, even at the strong interaction limit. Here, we also employ the equation of motion method. But, because of the on-site interaction term, this model cannot be solved exactly. After truncation of the high-order terms in the equation of motion, we get the retarded Green's function,[15,16]

$$G^r_\sigma(\omega)=\frac{1-\langle n_{\bar\sigma}\rangle}{\omega-\epsilon_\sigma-\Sigma^r_{0\sigma}(\omega)-\Sigma^r_{1\sigma}(\omega)}$$

with

$$\Sigma^r_{0\sigma}(\omega)=\sum_{k\in L,R}\frac{|V_{k\sigma}|^2}{\omega-\epsilon_{k\sigma}+i\eta},$$

$$\Sigma^r_{1\sigma}(\omega)=\sum_{k\in L,R}\frac{|V_{k\bar\sigma}|^2 f_{L/R}(\epsilon_{k\bar\sigma})}{\omega-\epsilon_\sigma+\epsilon_{\bar\sigma}-\epsilon_{k\bar\sigma}+i\eta}.$$

The self-energy $\Sigma^r_{0\sigma}(\omega)$ is the exact self-energy for the noninteracting case and does not depend on the temperature. The Kondo peak arises from the self-energy $\Sigma^r_{1\sigma}(\omega)$ when the temperature is lower than the Kondo temperature. The detail of the self-energy $\Sigma^r_{1\sigma}(\omega)$ and corresponding DOS of the quantum dot are given in Figs. 7 and 8. We note that the Kondo peak is very obvious when the temperature is low and the effects of the Van Hove singularities are the same as in the noninteracting case. This means that the Kondo peak and the peaks induced by Van Hove singularities may appear at the same time. Finally, we have to emphasize that in different experimental conditions the coupling constants can vary greatly, so that the effects of the singularities could be quite different. For instance, for the same molecules absorbed on different sites of the surface, due to the variation of the coupling constant, the peak induced by a Van Hove singularity may become a valley.

In conclusion, we have investigated the effect of Van Hove singularities in resonance tunneling. It will greatly affect the scanning tunneling spectroscopy measurements. The real part of the self-energy cannot be neglected any more; not only can it split the resonance peaks, but it also induces new peaks to the DOS. Thus we could not determine the positions of the discrete energy levels from the positions of the resonance peaks as with a metal tip. In particular, the first singularity above or below the Fermi energy gives rise to a very sharp peak even if the discrete energy level of the molecule is far from the Fermi energy. This kind of peak looks like the Kondo peak. But the scanning image, especially in a small scanning voltage, will be the same regardless of the kinds of probes being used. We expect that these phenomena could be observed in the STM experiments with nanotubes as the probes. Furthermore, the model we used here is quite general; we believe that these phenomena will exist in nearly all one-dimensional resonant tunneling experiments.

ACKNOWLEDGMENTS

We thank S. X. Du for helpful suggestions during the course of this work. We are also grateful to W. Ji, W. Guo, and H. Hu for their useful discussions and comments. This work is partially supported by the National Science Foundation of China, Chinese MOST "863" and "973" programs, and the Chinese Academy of Sciences. Q.F.S. is supported by the NSFC under Grants No. 90303016, No. 10474125, and No. 10525418, and X.C.X. is supported by the U.S. DOE under Grants No. DE-FG02-04ER46124 and No. NSF-CCF0524673.

[1] M. S. Dresselhaus, G. Dresselhaus, and Ph. Avouris, *Carbon Nanotubes: Synthesis, Structure, Properties, and Applications* (Springer, Berlin, 2001).

[2] H. Dai, J. H. Hafner, A. G. Rinzler, D. T. Colbert, and R. E. Smalley, Nature (London) **384**, 147 (1996).

[3] T. Shimizu, H. Tokumoto, S. Akita, and Y. Nakayama, Surf. Sci. **486**, L455 (2001).

[4] W. Mizutani, N. Choi, T. Uchihashi, and H. Tokumoto, Jpn. J. Appl. Phys., Part 1 **40**, 4328 (2001).

[5] Takashi Ikuno, Mitsuhiro Katayama, Masaru Kishida, Kazunori Kamada, Yuya Murata, Tatsuro Yasuda, Shin-ichi Honda, Jung-Goo Lee Hirotaro Mori, and Kenjiro Oura, Jpn. J. Appl. Phys., Part 2 **43**, No. 5A, L644 (2004).

[6] Shuji Hasegawa, The 4th International Workshop on Surfaces and Workshop on Water-surface Interactions, May 30, 2005, Beijing, China.

[7] R. Asito, G. Dresselhaus, and M. S. Dresselhaus, *Physical Properties of Carbon Nanotubes* (Imperial College Press, London, 1998).

[8] R. Saito *et al.*, J. Appl. Phys. **73**, 494 (1993).

[9] Bernhard Stojetz, Csilla Miko, Loazlo Forro, and Christoph Strunk, Phys. Rev. Lett. **94**, 186802 (2005).

[10] L. V. Keldysh, Sov. Phys. JETP **20**, 1018 (1965).

[11] D. C. Langreth, in *Linear and Nonlinear Electron Transport in Solids*, edited by J. T. Devreese and E. Van Doren (Plenum, New York, 1976).

[12] G. D. Mahan, *Many-Particle Physics* (Plenum, New York, 1990).

[13] H. Haug and A. P. Jauho, *Quantum Kinetics in Transport and Optics of Semiconductors* (Springer, New York, 1996).

[14] R. Saito, G. Dresselhaus, and M. S. Dresselhaus, Phys. Rev. B **61**, 2981 (2000).

[15] Y. Meir, N. S. Wingreen, and P. A. Lee, Phys. Rev. Lett. **66**, 3048 (1991).

[16] Y. Meir, N. S. Wingreen, and P. A. Lee, Phys. Rev. Lett. **70**, 2601 (1993).